Temperature-dependent order of clean Pd(110)

H. Hörnis, J. D. West, and E. H. Conrad
School of Physics, Georgia Institute of Technology, Atlanta, Georgia 30332

R. Ellialtioğlu
Department of Physics, Bilkent University, Ankara, 06533 Turkey
(Received 6 May 1993; revised manuscript received 2 August 1993)

We report high resolution low-energy-electron-diffraction measurements on the Pd(110) surface. We demonstrate that the clean surface consists of semiordered islands. The island structure is stable up to 650 °C at which point the island edges roughen and step-step correlations decrease. Above 1100 °C, surface evaporation becomes important and the surface becomes kinetically rough. A simple model is presented that makes use of step-step interactions to generate the periodic island structure. This model predicts that ordered islands form below the roughening temperature if the step creation energy is small compared to the step-step interaction. The existence of isolated steps is shown to be consistent with embedded atom calculations that predict a small step-formation energy on Pd(110) surfaces.

INTRODUCTION

The formation of surface defects such as steps, kinks, etc. have been actively studied over the last ten years.[1] These defects are present on miscut surfaces or on any surface above its roughening temperature T_R (T_R being the temperature where the free energy required to form a step becomes zero).[2] Since most models for roughening include only nearest-neighbor interactions, surfaces are predicted to be either rough or ordered. The role of long-range interactions, however, cannot be excluded in any serious discussion of equilibrium surface structures.

The addition of further nearest-neighbor interactions allows new types of disordered phases to form below T_R. Examples include the next-nearest-neighbor-induced prerough phase of den Nijs,[3] and the island structure caused by the asymmetry in the surface stress tensor between the 2×1 and 1×2 reconstructions on Si(001).[4] Long-range elastic interactions associated with defects have also been proposed to stabilize new ordered phases.[5]

The (110) surfaces of fcc metals are particularly interesting when discussing surface disorder because the $5d$ metal Au, Pt, and Ir(110) surfaces reconstruct into a 2×1 missing row reconstruction.[6] Theoretically these (110) surfaces can exist in flat, disordered flat (prerough), rough, or $(n\times1)$ reconstructed phases with a variety of continuous and first-order phase transitions between the different structures.[3,7] A good deal of experimental work has already been done on these surfaces.[1] For instance, Ni, Ag, Pb, In, and Cu(110) surfaces, which do not reconstruct, are all found to have roughening temperatures near $0.75T_m$ (T_m is the bulk melting temperature). On the other hand, Pt and Au(110) roughen at a significantly lower fraction of the melting point: $T_R/T_m \sim 0.5$, presumably due to the increased entropy on the more open missing row reconstruction.[1]

In this work we demonstrate that another type of disorder can be thermodynamically stable on (110) surfaces. Experimentally we find that the lowest-energy surface configuration for the clean Pd(110) surface over a wide temperature range is semiordered up-down steps. This surface is therefore intermediate between an ordered phase and a rough phase. We propose that this structure is stabilized by repulsive interactions between steps in much the same way that $(11m)$ surfaces of fcc metals have a stabilized ordered staircase structure.[1] This is quite different from experiments on Ag(110) that indicate that steps are attractive and lead to faceting.[8] We further suggest that the reason Pd(110) has such a disordered ground state is due to its proximity to the 1×1–2×1 reconstruction phase boundary as first suggested by den Nijs.[3]

EXPERIMENT

The experiments were performed in UHV (base pressure $<1\times10^{-10}$ torr) using a high-Q-resolution-low-energy, electron-diffraction (LEED) system with a transfer width of 8000 Å.[9] The sample was a 99.995% pure Pd single crystal spark cut and oriented to within 0.1° of the nominal ⟨110⟩ direction using a neutron diffractometer at University of Missouri Research Reactor. After mechanical polishing with 0.3-μm alumina powder, the sample was electropolished with a 50% sulfuric acid solution. The sample was mounted on a palladium foil and held with a palladium retaining ring to prevent any alloying with the sample holder. Sample temperatures were measured with a chromel-alumel thermocouple that was spot welded to a tantalum foil, which in turn was spot welded to the sample.

The Pd surface was cleaned *in situ* by ~1500 cycles of argon-ion sputtering at 500 eV for 10 min, followed by annealing at 1000 °C for 10 min. After cleaning, Auger spectra showed no C, S, or O contamination down to the noise limit of the analyzer (<1% of the Pd 320-eV Auger line). This cleaning procedure allowed the sample to be

kept at 1200 °C for 30 min and then cooled to room temperature with no change in the diffraction intensity. It was found that a well-ordered surface could only be obtained if the sample was annealed from 1000 to 400 °C in no less than 3 min.

The sample order was determined by measuring the specular $(\zeta,\zeta,0)$ crystal truncation rod (CTR) width as a function of Q_z, where Q_z is the component of the electron momentum-transfer vector normal to the surface. The scattering geometry is shown in Fig. 1(a). All of the diffraction data presented in this work are reported in the conventional bulk cubic reciprocal-lattice units $a^*(h,k,l)$, where $a^*=1.615$ Å^{-1}. The width of the specular diffraction rod was measured between the (110) and the (440) reciprocal-lattice points. The width was found to oscillate with a period $2\pi/c$, where c is a monoatomic step height on the Pd(110) surface ($c=2.75$ Å). This indicates that monoatomic steps are present on the Pd(110) surface even at room temperature.[10] Recent work by Yang *et al.* showed that double height steps form on Pb(110) just below its roughening temperature.[11] We found no evidence of step doubling on Pd(110) for sample temperatures between 30 and 1200 °C.

The reciprocal space width $\Delta Q_{\parallel}$ of the (440) peak is slightly broader than the (220) width. This is due to both the finite angular spread in the incident electron beam ($\Delta\theta_{\text{gun}}=0.07°$ at $E=300$ eV) and the surface mosaic $\Delta\theta_m$. When we deconvolve out the finite angular width of the electron beam, the sample mosaic spread is found to be $\sim 0.04°$. The finite domain size of the sample was determined from the width of the (220) peak ($\Delta Q_{\parallel}=0.008$ Å^{-1}). After deconvolving out both the transfer width of the instrument and the sample mosaic at the (220) position (0.006 Å^{-1}), the finite domain size for this Pd(110) surface was estimated to be >1200 Å.

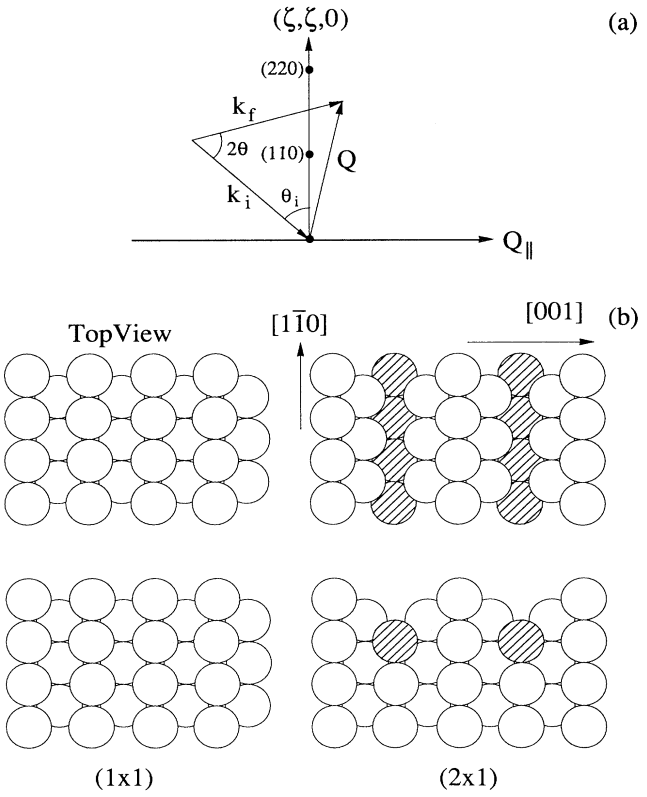

FIG. 1. (a) Scattering geometry for these experiments. The scattering angle 2θ is fixed and θ_i is rotated so that the scattered electron wave vector k_f is scanned across the $(\zeta,\zeta,0)$ rod. (b) Top and side views of an fcc (110) surface showing both 1×1 and 2×1 surface structures. The unit cell vectors for Pd(110) are $a_1=3.89$ Å and $a_2=2.75$ Å in the ⟨001⟩ and ⟨1$\bar{1}$0⟩ directions, respectively.

LOW-TEMPERATURE RESULTS

One of the main observations of this work is the appearance of strong satellite peaks near the specular rod for all sample temperatures below 1000 °C . This is shown in Fig. 2. The data were taken by measuring the diffracted electron intensity as a function of parallel momentum-transfer vector ($Q_{\parallel}$) through the (110) point on the specular rod. The bottom panel in Fig. 2 is a scan in the ⟨001⟩ direction [perpendicular to the atom rows; see Fig. 1(b)]. Distinct shoulders corresponding to several orders of diffraction can be seen around the $Q_{\parallel}=0$ diffraction rod. The satellite peaks occur in integer spacings of $\Delta Q_{\parallel}=n0.020\pm0.002$ Å^{-1}, and both $n=1$ and 2 orders can be resolved. Shoulders appear in the ⟨1$\bar{1}$0⟩ direction as well [parallel to the atom rows in Fig. 1(b)].

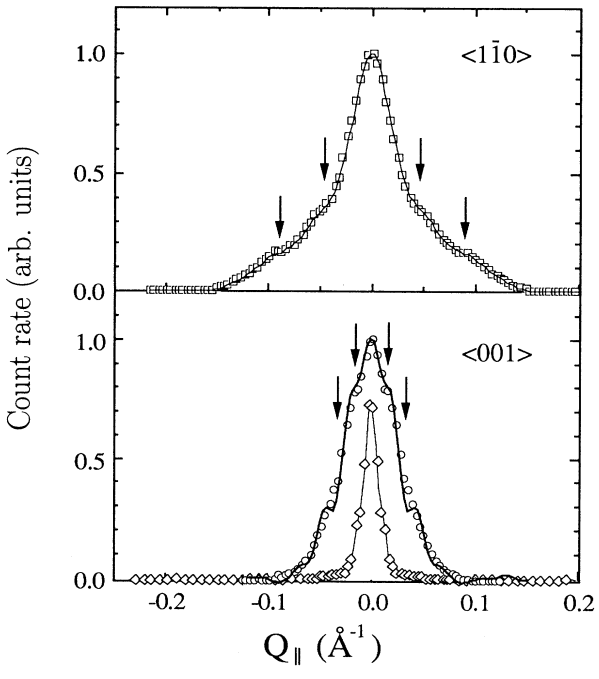

FIG. 2. $Q_{\parallel}$ scans through the (110) point taken both perpendicular to the atom rows, ⟨001⟩ (○) and along the rows, ⟨1$\bar{1}$0⟩ (□). For comparison, the (220) in-phase peak is shown (◇). The sample temperatures is 250 °C, electron energy is 307 eV, and the incident angle (relative to the sample normal) is 82.7°. Arrows indicate the positions of the satellite peaks. The solid line for the ⟨001⟩ azimuth is a fit as described in the text for $N=79$, $L=20$, and $m=59$.

In this direction the peak separations are larger; $\Delta Q_{\parallel}=n0.050\pm0.002$ Å^{-1}. It should be noted that the satellite peak separations are comparable to or less than the $Q_{\parallel}$ resolution of a typical LEED system ($\Delta Q_{\parallel}^{\mathrm{LEED}}>0.04$ Å). This explains why they have not been reported in the literature before now.

As shown in our previous work, the satellite peaks are instead consistent with a large-scale 80×45 reconstruction of the Pd(110) surface.[12] Within the experimental uncertainty ($\Delta Q_{\parallel}=\pm0.004$ Å^{-1}), the reconstruction was found to be independent of sample temperature from 50 up to 1000 °C, indicating that the surface structure responsible for the higher periodicity is very stable.[12] Although the periodicity of the structure is independent of temperature in this range, there is a temperature dependence of both the structure of the superlattice cell and its long-range order that will be discussed below.

The superlattice was found to be ordered over approximately 150–200 Å, corresponding to one or two superlattice cells. This is not a well-ordered superlattice structure. As we discuss below, however, the disorder of this large unit cell is most likely entropic and not an extrinsic property of the particular Pd sample that we used. This statement is supported by the fact that a potassium-induced Pd(110) 2×1 reconstruction on this same sample is as ordered as the sample finite size (>1200 Å).[13]

Because the satellite peaks only appear in a narrow range of Q_z's on the specular rod around the out-of-phase conditions [(110) and (330) reciprocal-lattice points], the superlattice structure has been identified as being due to ordered steps.[12] For $Q_z=4.56$ Å^{-1} corresponding to the (220) in-phase point on the specular diffraction rod, no shoulders are seen (see Fig. 2).

In order to estimate the structure of the stepped superlattice, we assume a simple one-dimensional (1D) model consisting of two levels separated by a monoatomic step as shown in Fig. 3(a). For convenience, the upper level will be referred to as the terrace and the lower level as the substrate. In this model the surface is assumed to consist of an ordered arrangement of up-down steps. The repeat distance between terraces is Na and the length of the upper terrace is ma (where N and m are integers). The amplitude scattered from the surface shown in Fig. 3(a) when there are p terraces is

$$A(\mathbf{Q})=\sum_{n_3=0}^{p-1} e^{in_3NaQ_{\parallel}}\left\{\sum_{n_1=0}^{m} e^{in_1aQ_{\parallel}}+\sum_{n_2=0}^{L-1} e^{i\{[(n_2+(m+\frac{1}{2})]aQ_{\parallel}-cQ_z\}}\right\}. \tag{1}$$

Note that the atomic positions parallel to the surface in the lower layer are shifted by $1/2a$ because of the fcc structure. Squaring Eq. (1) gives the peak intensity [$I(Q)=AA^*$]. The diffraction from this structure is a set of narrow reciprocal-lattice rods with a separation of $\Delta Q_{\parallel}=2\pi/Na$ (see Fig. 3).

The peak intensities of the satellite rods depend on the relative length of the terraces compared to the length of the exposed substrate. In the case where $m=N/2$, for example, there are an equal number of atoms in the terraces and the exposed substrate causing the specular intensity (at the out-of-phase condition) to be exactly zero.[10] Under these conditions, Eq. (1) predicts that the central peak is absent, leaving only two satellite peaks as shown in Fig. 3(b). As the size of the terrace or the exposed substrate shrinks (i.e., $m\neq N/2$), the specular intensity increases and the side peaks become weaker [Fig. 3(a)].

To compare our data to the line shapes predicted by Eq. (1), the calculated intensities must be convolved with the instrument function. This is done by assuming that the instrument is a Gaussian function with $\sigma=0.025$ Å^{-1} (σ is determined by both the instrument response and the measured sample mosaic). An example of a fit using Eq. (1) is shown in Fig. 2 for the $\langle 001\rangle$ azimuth. The fit is very good considering that we have not included any disorder in the island distribution. The fact that satellite peaks are observed, however, indicates that the distribution of terrace sizes must be peaked around some average size, implying some type of step-step interaction. In contrast, a noninteracting step model would produce a geometric distribution of terrace sizes resulting in a two-component line shape consisting of a sharp central peak centered on top of a broad Lorentzian background as shown in Fig. 3(c).[14] In other words a noninteracting step model would not predict satellite peaks.

Attempts to fit the scans in the $\langle 1\bar{1}0\rangle$ azimuth to Eq. (1) met with less success. As already mentioned, the calculation ignores any distribution of terrace sizes. By comparing the measured line shapes shown in Fig. 2 for the $\langle 001\rangle$ and $\langle 1\bar{1}0\rangle$ directions, it is obvious that in addition to weak satellite peaks the $\langle 1\bar{1}0\rangle$ direction has a

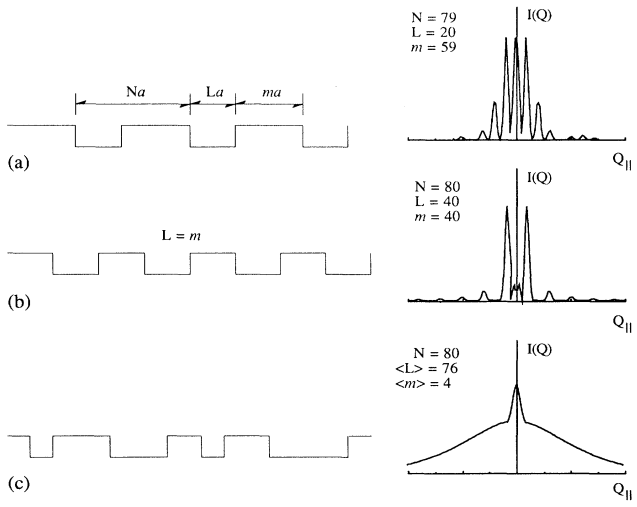

FIG. 3. (a) A two-level model of a stepped surface with a long-range periodicity of Na. Diffraction pattern for this surface is shown when $N=79$ and $m=59$. (b) An ordered stepped surface were $L=m$ and the corresponding diffraction pattern showing the missing central peak. (c) A random up-down surface with no long-range order.

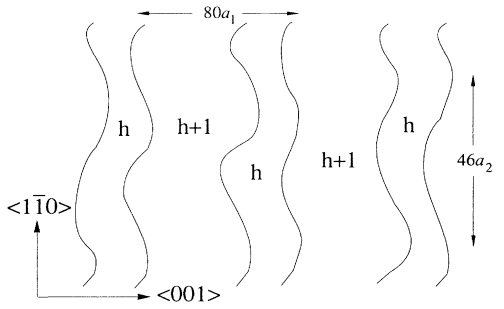

FIG. 4. Schematic representation of the low-temperature Pd(110) (1×1) surface as described in the text. The solid lines represent step edges separating the substrate (at a height h) and the terraces (at a height $h+1$).

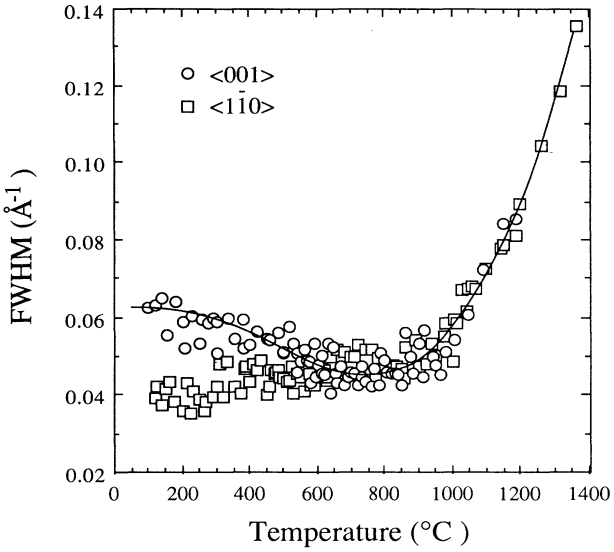

FIG. 5. FWHM of the (110) peak of Pd(110) vs temperature. The ○ and □ are for scans taken in the ⟨001⟩ and ⟨1$\bar{1}$0⟩ directions, respectively. The solid line is a guide to the eye for the ⟨001⟩ data. The electron energy is 307 eV, and the incident angle (relative to the sample normal) is 82.7° for all scans.

broad background component to its peak shape. In fact the ⟨1$\bar{1}$0⟩ data resemble the disordered step profiles shown in Fig. 3(c). We believe the ⟨1$\bar{1}$0⟩ line shapes are a result of low-energy kink excitations on the [001] steps. The broad tail is most likely due to fluctuations in the ⟨001⟩ step edges (i.e., step edge roughness) caused by kinks.

From the data discussed so far a structural model for the Pd(110) surface can be proposed. The surface consists of semiordered up-down steps perpendicular to the ⟨001⟩ direction (see Fig. 4). In addition to the steps forming a regular up-down array with an average repeat distance of 80 atoms in the ⟨001⟩ direction, the step edges fluctuate with a period of about 46 atoms. The step edge waving may be similar to that observed on Si(001).[15] So far we have not quantitatively addressed the question of the terrace size relative to step-step separation (other than to show that they are not equal). This is because the ratio of m/L is a function of temperature, as will be shown in the next section.

TEMPERATURE DEPENDENCE

While the satellite peaks remain visible and their separation stays constant up to 1000 °C, the line shapes have an appreciable temperature dependence that is due to a change in the relative intensity of the central peak to the satellite peaks. To demonstrate the temperature dependence we have plotted the peak full width at half maximum (FWHM) versus temperature in Fig. 5. We have plotted the FWHM instead of the peak ratios because the peak separations are small compared to the mosaic broadening (at least in the ⟨001⟩ direction). This makes accurate determinations of the m/L ratios difficult. The FWHM is more easily measured and, as we show below, it is related to the peak ratios. Qualitatively, for scans in the ⟨001⟩ direction, the FWHM increases when the central peak intensity decreases relative to the satellites. Likewise, when the central peak intensity increases, the FWHM decreases.

From Fig. 5, three temperature regions can be identified where the surface structure changes. The structures in all three temperature regions are completely reversible. The line shapes are essentially constant up to 500 °C, at which point they change substantially. Between 500 and 900 °C the FWHM in the [001] direction, perpendicular to the atom rows, decreases, indicating that the side peaks become less intense relative to the central peak. In the [1$\bar{1}$0] directions the FWHM increase is due mostly to an increase in the broad background component of the line shape. Since the separation distance between satellite peaks does not change in the temperature range 500–900 °C, the superlattice period remains constant. Therefore, the changes in the FWHM indicate a rearrangement of the structure of the superlattice cell.

To be more quantitative, we use the fact that the ratio of the specular peak intensity to the side peak intensity is proportional to the relative size of the upper and lower layers, which in turn is proportional to the measured FWHM. To estimate the mean terrace width from the FWHM of the ⟨001⟩ peak profiles, we calculated the line shapes as a function of m_1/L_1 based on the model structure leading to Eq. (1). These calculated line shapes were convoluted with the instrument response function. Once this was done, a table of calculated FWHM vs m_1/L_1 was generated from these calculated peak shapes. Using this table, the experimental FWHM of the ⟨001⟩ peaks were converted to m_1/L_1. The results are shown in Fig. 6(a).

Up to 600 °C the ratio of the terrace size to step separation is nearly constant at $m_1/L_1=0.42$ for the steps in the ⟨001⟩ direction. By 600 °C the ratio decrease to $m_1/L_1=0.30$, and again remains constant up to 1000 °C. It must be noted that the y axis in Fig. 6(a) could equally

be L_1/m_1 instead of m_1/L_1. The diffraction data do not allow us to determine whether there are more or less atoms in the terraces compared to the substrate—it can only determine the ratio. However, as discussed below, the temperature dependence of m_1/L_1 suggests that the terraces are smaller than the exposed substrate.

In the $\langle 1\bar{1}0 \rangle$ direction the FWHM increases slightly between 500 and 800 °C (see Fig. 5). The increase is due entirely to a change in the ratio of the central peak to the broad Lorentzian background component in the line shape. In a two-level system with random steps [see Fig. 3(c)] the ratio between the broad background (Lorentzian) and the central peak, $I_{\text{Lor}}/I_{\text{peak}}$, is a function of the coverage of terrace atoms: $\theta = L_2/N_2$,[16]

$$\frac{I_{\text{Lor}}}{I_{\text{peak}}} = \frac{2[1-\cos(Q_z c)]}{\frac{\theta}{1-\theta}+\frac{1-\theta}{\theta}+2\cos(Q_z c)}, \tag{2}$$

where c is the step height in the $\langle 110 \rangle$ direction ($c = 2.75$ Å). Using the experimental ratios of the background to peak ratios, we have plotted L/N for the $\langle 1\bar{1}0 \rangle$ direction in Fig. 6(b). From Fig. 6(b), it is seen that as the terrace m_1 in the $\langle 001 \rangle$ direction decreases at 600 °C, the average separation between defects on the $\langle 1\bar{1}0 \rangle$ direction also decreases.

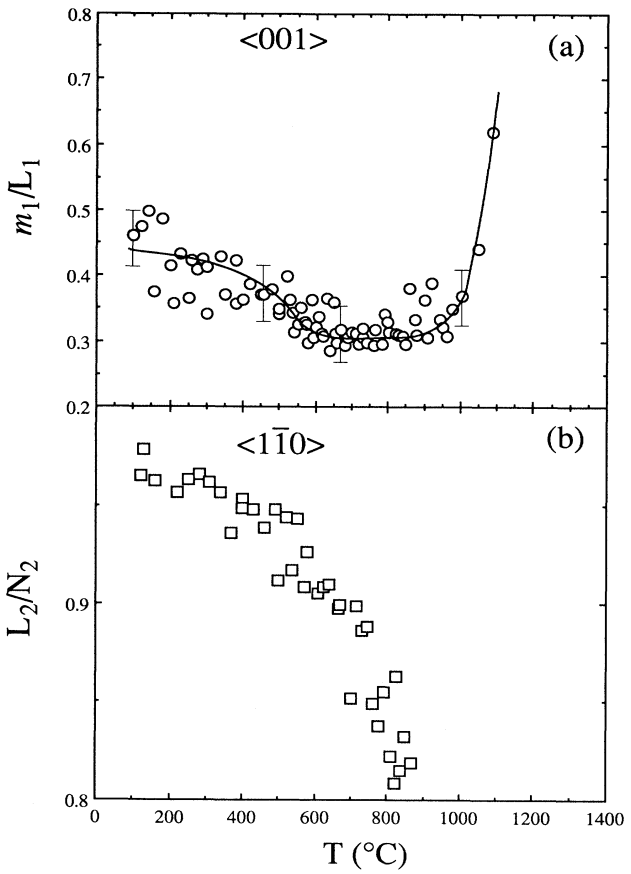

FIG. 6. (a) The ratio of the terrace width m and terrace separation L vs temperature for the $\langle 001 \rangle$ direction. The solid line is a guide to the eye. (b) The ratio of the average kink separation L and the average distance between step fluctuations N in the $\langle 1\bar{1}0 \rangle$ direction.

We propose that the temperature dependence of the diffraction data can be interpreted as step edge roughening at 600 °C due to the formation of kinks and/or adatoms dissolving from the step edges in the $\langle 001 \rangle$ direction. At 600 °C the increased entropy associated with either kinks or adatoms overcomes the step-step interactions. The [001] step edges meander so that the average distance between kinks in the $\langle 1\bar{1}0 \rangle$ direction decreases. The decreasing correlation between step edge atoms along the [001] steps causes the $\langle 1\bar{1}0 \rangle$ line shapes to broaden. When kinks form, the $\langle 001 \rangle$ step edges move $\pm a_1$ in the $\langle 001 \rangle$ direction, and the distribution of terrace sizes is expected to broaden so that the satellite peak intensity would decrease. This in turn would cause a narrowing of the diffraction line shapes in the $\langle 001 \rangle$ direction consistent with Fig. 5. Adatoms dissolving from the step edges would additionally cause the average terrace size to shrink (since scattering from the adatoms does not contribute to the line shape, only to the background intensity), which is also consistent with the data in Fig. 6(a). That is, at higher temperatures we expect that entropy will tend to break up larger terraces into smaller ones. It is for this reason that we believe the data in Fig. 6(a) are plotted correctly. We do not expect the terraces to grow large at higher temperatures simply from entropy arguments. A possible exception to this argument is that a strain in the surface layer due to a differential thermal-expansion coefficient between the bulk and the surface could favor larger terraces.

If the distribution of superlattice cells becomes broader as kinks from above 600 °C, we would also expect that the side peak width would also broaden in this temperature range. It is difficult to say whether or not this is happening because the peaks are so closely spaced and comparable in width to the sample mosaic broadening.

Above 1100 °C, the line shapes change again, indicating another transformation in the surface morphology. Above this temperature the satellite peaks disappear and the entire line shape begins to broaden. Once again the broadening is associated only with the out-of-phase diffraction peaks; (220) and (440) peaks show no change in shape. At first glance, the loss of any long-range order in the superlattice and the increased peak widths is consistent with a roughening transition.[1,17] If we assign the roughening temperature to be 1100 °C, the ratio of the roughening temperature to the bulk melting temperature would be $T_R/T_m = 0.75$. This ratio is similar to those measured for the roughening of Ni, Cu, Ag, Pd, Al, and In(110) surfaces. For these materials T_R/T_m ranges between 0.8 and 0.69.[1] However, the assumption that the line-shape broadening above 1000 °C is due entirely to a surface roughening transition must be viewed with some caution when Pd's vapor pressure is considered. Between 800 and 1000 °C, Pd's vapor pressure increase from 1.2×10^{-9} to 8.4×10^{-7} torr.[18] By 1100 °C the evaporation rate is approximately 1.0 monolayer/sec. Therefore the roughness indicated by the increasing linewidth above 1100 °C is not completely thermodynamic in origin but contains some short-range dynamic roughness.[19] For

purely dynamic roughening, the linewidths at a fixed temperature would be time dependent but saturate to a fixed value at $t \rightarrow \infty$. An estimate based on previous dynamic roughness studies during growth would suggest that typical saturation times are on the order of 1–2 h for a 2-monolayer/sec evaporation rate.[20] This is much longer than the time between typical data points in Fig. 5. Since no hysteresis was observed in the line-shape measurements above 1000 °C, a steady-state dynamic roughness was not achieved in these experiments.

DISCUSSION

We now propose a model that can rationalize the low-temperature island structure observed on this surface. For simplicity we ignore the crystallographic anisotropy and consider an ordered array of $p \times p$ square islands on a flat substrate $M \times M$ atoms wide. Each island contains $m \times m$ atoms. The distance between adjacent island boundaries is La (where L is an integer and $M = p[m + L]$). The free-energy difference between an island covered surface and a flat surface without islands will be

$$\Delta F = \gamma 4mp^2 \pm mp^2\sigma \left[\frac{1}{L^2} + \frac{1}{m^2} \right] . \quad (3)$$

The first term in Eq. (3) is the step energy per unit length of the island perimeter, γ. The second term is the step-step interaction energy that has contributions from interisland and intraisland step edges. The step-step interaction is presumed to be elastic (rather than entropic) in origin.[21] Contributions to Eq. (3) that arise from the configurational entropy of the islands are neglected in this simple treatment, but we will comment on them below.

For attractive steps [minus sign in Eq. (3)], the steps will bunch and the crystal will facet into flat(110) planes coexisting with high index stepped regions.[22] We will not concern ourselves with attractive steps since we find no evidence of surface faceting on Pd(110). Evidence of faceting on Ag(110), however, does exist.[8]

For repulsive steps, this model predicts that ΔF will always have a minimum for some combination of L and m if $\gamma < 0$. In other words, ordered steps will be preferred over the flat surface. The L and m values leading to a minimum in ΔF are found by setting both differentials $(\partial \Delta F / \partial m)_l$ and $(\partial \Delta F / \partial L)_m$ equal to zero with the constraint that $M = p[m + L]$ is a constant. Solving these two simultaneous equations for $L_{\min}$ and $m_{\min}$ gives the result that the minimum in ΔF occurs at an m/L ratio that is independent of either γ or σ and depends only on the form of the step-step repulsion. For a L^{-2} repulsive potential $(m/L)_{\min} = 1.78$, and for an L^{-1} repulsive potential $(m/L)_{\min} = 2.00$. These values will also change when asymmetry is added to the model. For instance a purely 1D model consisting of straight steps running in only one direction gives $(m/L)_{\min} = 1.00$ regardless of the form of the step-step potential. Of course the size of an island will depend on γ and σ. Since no accurate estimates for these coefficients exist, we have not attempted to calculate an estimate of the island size.

As already stated, in order for the free energy to have a minimum, the condition $\gamma < 0$ must be met. In the absence of step-step interactions, the condition that the step free energy is less than zero implies that the surface is above its roughening temperature and that ordered islands cannot exist.[2] But we argue that a long-range step repulsion renormalizes the step free energy, and has the effect of raising the roughening temperature so that ordered steps can still exist at finite temperatures. This is completely analogous to the situation of vicinal metal surfaces where an ordered step staircase exists because of step-step interactions.[23] On these surfaces T_R increases as the step-step interaction increases (i.e., as the terrace length between steps decreases).[1] Experiments on Cu(11m) and Ni(11m) surfaces confirm this trend.[24]

Whether or not the structure we propose is favorable depends crucially on Pd(110) having a small step energy. The (110) fcc metals are rather unique because some of them (Au, Pt, Ir) have a 2×1 missing row reconstruction.[6] The nature of this reconstruction is important to this work. The (110) 2×1 surface is essentially an ordered arrangement of steps (see Fig. 1). The energy difference $\Delta E_{2\times1}$ between the 2×1 and 1×1 surfaces is therefore closely related to the energy cost to produce a step. The reconstruction energy has been calculated by several groups using embedded atom potentials.[25] It is found that $\Delta E_{2\times1}$ for Pd and Ag(110) is either small or negative, indicating that the cost of making a step on these surfaces is low (at least as predicted by these models). So it seems reasonable to assume that γ for Pd(110) may indeed be small. At finite temperatures the entropy associated with step formation will further lower γ.

We note that den Nijs *et al.* suggested that if the energy to make a step is low on a (110) surface, and if next-nearest-neighbor interactions are strong enough, the surface can become "prerough."[3] The prerough phase is flat (a finite height-height correlation function) with no long-range order, but does consist of a series of correlated up-down steps. That is, every up step is followed by a down step. For 1D steps, the prerough phase has $m/L = 1.0$ (for 2D square islands $m/L = 0.71$). The restricted solid-on-solid model that leads to the prerough phase assumes that long-range interaction can be ignored and that only first- and second-neighbor interactions are important. The fact that our experiments determine $m/L < 1.0$ may suggest that the Pd(110) surface is always in a state similar to the prerough phase. However, some long-range order still remains up to 1000 °C. Indeed, on Pd, and probably on most metal surfaces, step-step interactions may prevent a true prerough phase from forming.

ACKNOWLEDGMENTS

We wish to thank Professor A. Zangwill for suggesting the possible importance of step-step interactions to this problem. This work has been supported by the NSF under Grant No. DMR-9211249, Petroleum Research Foundation No. 23741-AC5, and by a NATO travel grant.

[1]For a review see, Edward H. Conrad, Prog. Surf. Sci. **39**, 65 (1992).
[2]H. van Beijeren and I. Nolden, in *Structures and Dynamics of Surfaces,* edited by W. Schommers and P. von Blanckenhagen (Springer, Heidelberg, 1987).
[3]M. den Nijs, Phys. Rev. Lett. **64**, 435 (1990).
[4]O. L. Alerhand, D. Vanderbilt, R. D. Meade, and J. D. Joannopoulos, Phys. Rev. Lett. **61**, 1973 (1988); F. K. Men, W. E. Packard, and M. B. Webb, *ibid.* **61**, 2469 (1988).
[5]Dieter Wolf, Phys. Rev. Lett. **70**, 627 (1993).
[6]W. Moritz and D. Wolf, Surf. Sci. **163**, L655 (1985); I. K. Robinson, Phys. Rev. Lett. **50**, 1145 (1983); L. D. Marks, *ibid.* **51**, 1000 (1983); M. Copel and T. Gustafson, *ibid.* **57**, 723 (1986); E. C. Sowa, M. A. van Hove, and D. L. Adams, Surf. Sci. **199**, 174 (1988); G. L. Kellog, Phys. Rev. Lett. **55**, 2168 (1985); P. Ferry, W. Moritz, and D. Wolf, Phys. Rev. B **38**, 7275 (1988); **38**, 7275 (1988), and references therein.
[7]J. Villain and I. Vilfan, Surf. Sci. **199**, 165 (1988).
[8]I. K. Robinson, E. Vlieg, H. Hörnis, and E. H. Conrad, Phys. Rev. Lett. **67**, 1890 (1991).
[9]Y. Cao and E. H. Conrad, Rev. Sci. Instrum. **60**, 2642 (1989).
[10]M. Henzler, in *Electron Spectroscopy for Surface Analysis,* edited by H. Ibach (Springer, Berlin, 1979).
[11]H.-N. Yang, K. Fang, G.-C. Wang, and T.-M. Lu, Europhys. Lett. **19**, 215 (1992).
[12]H. Hörnis, J. West, E. H. Conrad, and R. Ellialtioğlu, Phys. Rev. B **47**, 13 055 (1993).
[13]H. Hörnis and E. H. Conrad (unpublished).
[14]C. S. Lent and P. I. Cohen, Surf. Sci. **139**, 121 (1984).
[15]J. Tersoff and E. Pehlke, Phys. Rev. Lett. **68**, 816 (1992).
[16]C. S. Lent and P. I. Cohen, Surf. Sci. **139**, 121 (1984).
[17]See J. D. Weeks, in *Ordering in Strongly Fluctuating Condensed Matter Systems,* edited by T. Riste (Plenum, New York, 1980).
[18]*Smithells Metal Reference Book,* 6th ed., edited by E. A. Branges (Butterworths, London, 1983).
[19]For a review, see F. Family, Physica (Amsterdam) **168A**, 561 (1990).
[20]Y.-L. He, H.-N. Yang, T.-M. Lu, and G.-C. Wang, Phys. Rev. Lett. **69**, 3770 (1992).
[21]A. F. Andreev and Yu. A. Kosevich, Zh. Eksp. Teor. Fiz. **81**, 1435 (1981) [Sov. Phys. JETP **54**, 761 (1981)].
[22]H. J. Schultz, J. Phys. (Paris) **46**, 257 (1985).
[23]J. Villain, D. R. Grempel, and J. Lapujoulade, J. Phys. F **15**, 809 (1985).
[24]F. Fabre, B. Salanon, and J. Lapujoulade, in *The Structure of Surface II,* edited by J. F. van der Veen and M. A. Van Hove (Springer, Berlin, 1988), p. 520; E. H. Conrad, L. R. Allen, D. L. Blanchard, and T. Engel, Surf. Sci. **187**, 265 (1987).
[25]S. M. Foiles, Surf. Sci. **191**, L779 (1987); S. P. Chen and A. F. Voter, Surf. Sci. Lett. **244**, L107 (1991).